ACS APPLIED MATERIALS & INTERFACES

Research Article

www.acsami.org

Copolymer Coatings Consisting of 2-Methacryloyloxyethyl Phosphorylcholine and 3-Methacryloxypropyl Trimethoxysilane via ATRP To Improve Cellulose Biocompatibility

Bo Yuan,[†] Qiang Chen,*[,†,‡] Wen-Quan Ding,[†] Ping-Sheng Liu,[†] Shi-Shan Wu,[†] Si-Cong Lin,[†] Jian Shen,*[,†] and Yue Gai[†]

[†]School of Chemistry and Chemical Engineering, Nanjing University, Nanjing 210093, People's Republic of China

[‡]High Technology Research Institute of Nanjing University, Changzhou 213164, People's Republic of China

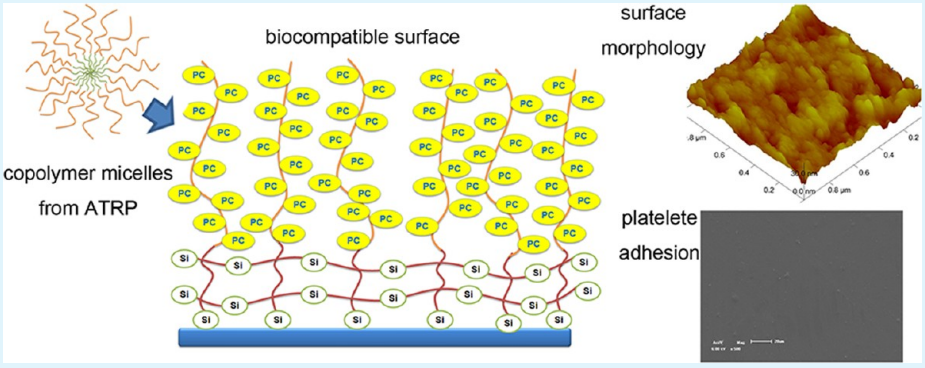

ABSTRACT: AB diblock copolymers comprised of poly(2-methacryloyloxyethyl phosphorylcholine) (PMPC) and poly(3-methacryloxypropyl trimethoxysilane) (PMTSi) segments, which are used for biocompatible coatings, were investigated. Block copolymers with various compositions were synthesized by atomic transfer radical polymerization (ATRP). The obtained copolymers were dissolved in an ethanol solution, and dynamic light scattering showed that all block copolymers were capable of existing as micelles. After a convenient "one-step" reaction, the cellulose membranes could be covalently modified by these copolymers with stable chemical bonds (C−O−Si and Si−O−Si). Block copolymers with different PMPC chain length were applied to surface modification to find the most suitable copolymer. The functional MPC density can be controlled by adjusting the ratio of the two monomers (MPC and MTSi), which also affect surface properties, including the surface contact angle, surface morphology, and number of functional PC groups. The low-fouling properties were measured by protein adsorption, platelet adhesion and activation, and cell adhesion. Protein adsorption of bovine serum albumin (BSA), fibrinogen, and human plasma were also tested and a moderate monomer composite was attained. The protein adsorption behavior on the novel interfaces depends both on MPC density and PMPC chain length. Platelet adhesion and activation were reduced on all the modified surfaces. The adhesion of Human Embryonic Kidney 293 (293T) cells on the coated surfaces also decreased.

KEYWORDS: *biocompatibility, ATRP, copolymer, micelles, cellulose, surface modification*

INTRODUCTION

The most important factor that distinguishes a biomaterial from any other material is its ability to exist while in contact with human body tissue without causing an unacceptable degree of harm to that body. Thus, the biocompatibility is a critical issue of implanted biomedical devices, especially when it comes to the body fluid contact aspect. Surface modification is an effective method to improve the blood compatibility of the usual substrates, which are transplanted into human bodies.[1]

2-Methacryloyloxyethyl phosphorylcholine (MPC) polymers have been widely used to construct nonbiofouling surfaces in various medical applications, because they have been proven to resist both protein adsorption and cell adhesion.[2−7] The MPC unit contains a zwitterionic phospholipid group (i.e., phosphorylcholine (PC)), present in cell membranes and possessing nonthrombogenic properties and high biocompatibility. Main methods that use this promising chemical are blending,[8,9] copolymerization,[5,9−12] and surface modification.[2,3,10−12] MPC has been widely used to resist protein adsorption and cell adhesion in various substrates such as cellulose,[13,14] polysulfone,[15] polyurethane,[16,17] and metals.[11,12]

There are two general approaches for graft polymerization: "grafting to" methods[2,3,11,12] and "grafting from" methods.[13,18] In the "grafting from" process, chains grow from initiating sites on the surface; this is also known as surface-initiated grafting polymerization. Although high grafting density is achievable,

Received: May 13, 2012
Accepted: August 2, 2012
Published: August 2, 2012

   dx.doi.org/10.1021/am3008399 | *ACS Appl. Mater. Interfaces* 2012, 4, 4031−4039

difficulties in grafted chain characterization are obvious.[19] Moreover, surface-initiated atomic transfer radical polymerization (ATRP) requires a surface-activating step at first; consequently, the ensuing propagation demands strict control.

On the other hand, the "grafting to" method leads to great advantages, in which part of the polymer chains bear reactive moieties while the other parts are covalently attached to reactive surfaces. The premade grafted chains can be well-characterized before attachment. Compared to surface-initiated grafting polymerization, the grafting density during this process is lower, because earlier-grafted chains will prevent later-grafted chains from approaching to the substrate surface. Despite the strict experimental conditions that control the polymerization process, the "grafting to" approach behaves in a more convenient way within the surface modification area.[11,19]

Recently, more evidence has been accumulated that polymer brushes exhibit much lower protein adsorption, not only from single-protein solutions but also from human blood plasma. Furthermore, the polymer brushes, of which the number of bioactive molecules binding sites can be controlled, effectively enhance the surface antifouling properties, as a result of the high functional group density at the brush interface.[20,21]

ATRP is a facile and effective method to design and prepare novel block copolymers with functional groups. The silicone monomer employed was 3-methacryloxypropyltrimethoxysilane (MTSi). Because of its high activity of silanol groups of alkoxysilane, premature hydrolysis and cross-linking reactions of this chemical must be avoided to obtain stable micelles with traces of water. However, chain blocks with decades of high-activity functional groups will provide stable adhering layers with C−O−Si bonds, from silylation reaction with the surface hydroxyl and Si−O−Si bonds from interconnection.

These novel diblock copolymers with multiactivated-plots can react easily under moderate environment with hydroxyl groups on carbohydrate, metals, and alloys, which have been widely applied in clinical medical devices such as hemodialyzers, orthopedic screws, contact lenses, surgical sutures, and medical gauze. Biofouling is inevitable when these artificial medical devices come into contact with human fluids. Thus, the requirement of antiprotein-adsorption and anticoagulation is quite urgent. Through this research, we offer an effective and convenient method to produce low-fouling medical devices in the short term, in which the synthesized copolymers are promising for widespread application in surface modification.

EXPERIMENTAL SECTION

Materials. MPC (Nanjing Joynatural Institute of Science and Technology, 99%) was used without further purification. MTSi (Nanjing Yudeheng Fine Chemical Co., Ltd., 98%) was distilled before use. Ethyl 2-bromoisobutyrate (EBIB, Alfa Aesar, 98%), *N*,*N*,*N*′,*N*″,*N*″-pentamethydiethylenetriamine (PMDETA, Aladdin-Reagent, 98%), 2,2′-bipyridine (bpy), tetrahydrofuran (THF), petroleum ether, methanol, and ethanol (with dehydration) were obtained from Sinopharm Chemical Reagent Co. Ltd. Copper(I) bromide (CuBr) were stirred with glacial acetic acid, later washed consecutively with glacial acetic acid, acetone, and dried with rotary distillation. Cellulose membranes (CMs) were purchased from Sigma−Aldrich, then cut into circular pieces and washed in ethanol several times using an ultrasonic cleaning instrument.

Synthetic Procedures of PMTSi. A typical ATRP in ethanol was carried out as follows: MTSi (3.3 g, 13.4 mmol, 20 equiv), EBIB (0.52 g, 2.68 mmol, 4 equiv) and PMDETA (0.23 g, 1.34 mmol, 2 equiv) were dissolved into 3 mL of dehydrated ethanol (bubbled with argon gas for 1 h to remove traces of oxygen). After three freeze−pump−thaw cycles, CuBr (0.096 g, 0.67 mmol, 1equiv) was added into the solution under nitrogen atmosphere and then the entire system was pumped to vacuum. After immersion into a 60 °C oil bath for 24 h, the mixture solution was exposed to air to halt the reaction and the solution viscosity increased through the reaction process. (See Scheme 1.) Copper bromide was removed using an Al_2O_3 column and

Scheme 1. Molecular Formula and Reaction Route of the Copolymers

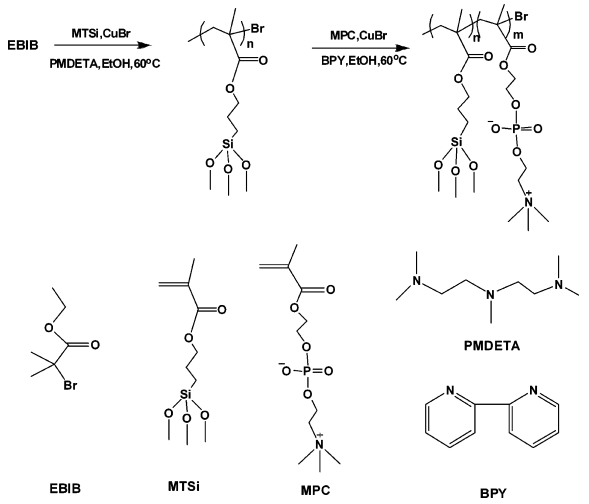

petroleum ether was added afterward (three times) to remove the monomers and residual initiators. Characterization was made via ^{1}H NMR in deuterated chloroform: δ_H = 0.51−0.67 ($\alpha-CH_3$), 0.73−0.84 ($-CH_2Si$), 0.92−1.01 ($-CH_2-$, backbone), 1.59−1.74 ($OCH_2-CH_2-CH_2Si$), 3.45−3.60 ($-SiO(CH_3)_3$), 3.78−3.93 ($-COO-CH_2$).[22,23]

Polymerization of PMTSi-b-PMPC. The protocol of preparing diblock copolymers with different PMPC blocks involved the following: PMTSi (0.15 g, number-average molecular weight of M_n = 3500, 0.042 mmol), MPC (0.179 g, 0.6 mmol; 0.358 g, 1.2 mmol; 0.638 g, 2.1 mmol; 0.894 g, 3 mmol; 2.55 g, 8.6 mmol), CuBr (0.096 g, 0.67 mmol), and bpy (0.209 g, 1.3 mmol) in dehydrated ethanol (bubbled with argon gas for 30 min to remove traces of oxygen before). The reaction lasted for 12 h, and final products were preserved in the ethanol above. Characterization by ^{1}H NMR in methanol-D4 revealed the following: δ_H = 0.60−0.76 ($-CH_2Si-$), 0.88−1.13 ($\alpha-CH_3$), 1.20−1.32 ($-CH_2-$, backbone), 1.70−1.84 ($OCH_2-CH_2-CH_2Si$), 3.18−3.43 ($-N(CH_3)_3$), 3.71−3.81 ($-CH_2N$), 3.83−3.95($-COOCH_2-CH_2CH_2Si-$), 4.04−4.30 ($-OCH_2CH_2OP$), and 4.30−4.45 ($-POCH_2-$).[12]

Surface Modification. The block copolymers were referred as *n*-*m* (where *n* represents the degree of PMTSi polymerization measured by GPC, while *m* represents the degree of PMPC polymerization in design). These were diluted by ethanol to make a series of solutions with a volume of 100 mL; 1% (v/v) triethylamine (TEA) was also added to catalyze the process. The membranes were immersed into the solution for 5 h at 60 °C.[22] The modified CMs were then washed by ethanol and water consecutively three times (see Scheme 2).

Platelet Adhesion and Platelet Activation. The substrates were placed in individual wells of a 24-well tissue culture plate and equilibrated with PBS overnight. Five hundred microliters (500 μL) of platelet-rich plasma (PRP) was added into each well and incubated at 37 °C for 120 min under static conditions. After being rinsed with PBS three times, the substrates were immersed into 2.5% glutaraldehyde in PBS for 30 min, which was subjected to a series of graded alcohol−water solutions (25%, 50%, 75%, 95%, and 100%) for 20 min in each step and dried under vacuum. Finally, the substrates, after they were coated with gold, were examined and photographed using a scanning electron microscopy (SEM) system (Shimadzu, Model SSX-550).[24]

Pristine CMs and CMs modified with different copolymers were immersed with 500 μL of PRP at 37 °C for 120 min. Fifty microliters

Scheme 2. Modification of the Cellulose Membrane (CM) in the Copolymer Solutions

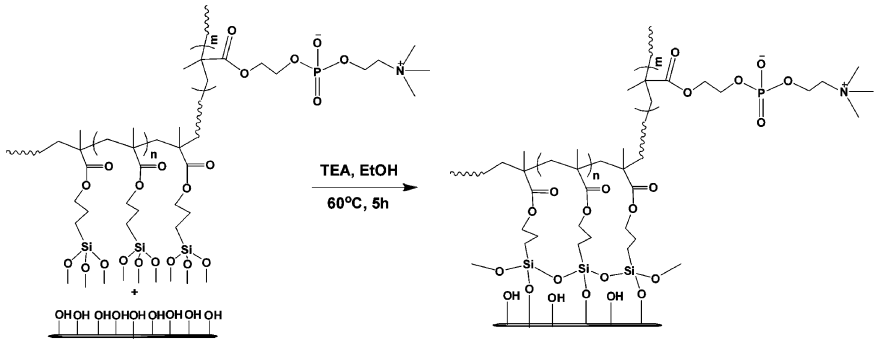

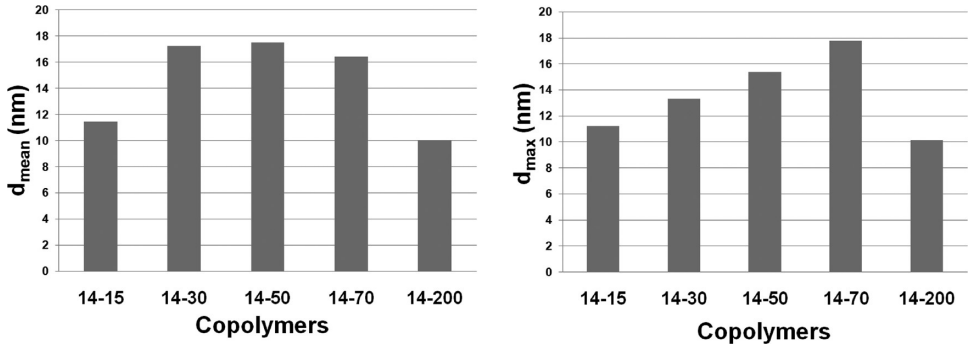

Figure 1. Trend graph of mean article size (d_{mean}) versus copolymers (left panel) and maximum particle size (d_{max}) versus copolymers (right panel).

(50 μL) of PRP from each well was then added into a 96-well tissue culture plate in an ELISA kit. The soluble p-selectin released from activated platelets was evaluated by an enzyme-linked immunosorbent assay (ELISA, ElabScience, Wuhan, China).

Protein Adsorption. After being equilibrated with PBS overnight, the CM substrates were immersed in 2 mL of protein solutions (1.5 mg/mL BSA or fibrinogen, with platelet-poor plasma (PPP) from human plasma[25]) at 37 °C for 90 min and then rinsed with PBS three times. The adsorbed protein was detached by immersing the substrates in 1% SDS for 60 min and concentration of the adsorbed protein was determined by bicinchoninic acid (BCA) (BCA Protein Assay Kit, Thermo) method at wavelength of 562 nm. Independent measurements were performed in at least triplicate samples, and the total amounts of the adsorbed proteins were calculated from the concentration of the standard protein solution.[13,26]

Adhesion of Human Embryonic Kidney 293 (293T) Cells. The substrates were placed in dishes and under UV radiation for 60 min, and then they were placed into a 48-well tissue culture plate. Human Embryonic Kidney 293 (293T) cells (1.5×10^5) were added into the wells. The plate was incubated for an hour at 37 °C under a carbon dioxide (CO_2) pressure of 5%. The substrates were then washed by PBS three times and digested by 0.25% trypsin and counted.

Analysis and Measurements. *Gel Permeation Chromatography.* The PMTSi molecular weight distribution was determined by gel permeation chromatography (GPC). GPC measurements were carried out at room temperature, using a device that was equipped with STYRAGEL HR3, HR4, and HR5 columns (300 × 7.8 mm) from Waters. A Waters 2487 Ultraviolet absorbance detector and a Wyatt Technology Optilab rEX refractive index detector were used to obtain the results. THF was used as eluent at a flow rate of 1 mL/min. Calibration was done using polystyrene (PS) standards, and the molecular weights were calculated within the range from 900 g/mol to 1.74×10^6 g/mol (with NMD for 1.02−1.11).

Nuclear Magnetic Resonance (NMR). The polymerization process was monitored by a Bruker 300 ULTRA SHIELD spectrometer (300 MHz) ^{1}H NMR. PMTSi polymers were dissolved in deuterated chloroform, and the copolymers were dissolved in deuterated methanol-D4.

Micelles Diameter in Solution by Dynamic Light Scattering (DLS). The measurement was performed at a scattering angle of 90°, equipped with a Brookhaven Instruments BI-200SM goniometer in a solution of 1% w/v copolymer/ethanol with a 75 mW Melles Griot He−Ne laser (wavelength 632.8 nm). All dynamic light scattering (DLS) measurements were conducted at 25 °C. Data regarding the distribution of intensity, relative to diameter, were collected.

Surface Characterization of Cellulose Membranes (CMs). All X-ray spectroscopy measurements were recorded on a VG Scientific ESCALAB MK-II spectrometer using Al Kα source run at 15 kV and 10 mA. The binding energy scale was calibrated to 284.6 eV for the main C 1s peak. Each sample was analyzed at a 90° angle, relative to the electron analyzer.

Static water contact angle (SCA) detection was measured on a DataPhysics instrument (Model OCA-30, Germany). One drop of water (3 μL) was put on the film surface with an automatic piston syringe and photographed.

The surface morphology of the substrates was observed by an atomic force microscopy (AFM) of Veeco DI Nanoscope Multimode. A piece of properly sized dry substrate was placed on a clean iron wafer and observed in tapping mode with 1 Hz.

RESULTS AND DISCUSSION

Preparing the Diblock Copolymer Coatings with Phospholipid. PMTSi-Br macromolecular initiator was prepared with PMDETA and purified first. The monomer conversion of the reaction was more than 99% by ^{1}H NMR at 60 °C for 24 h. The dispersity was 1.35, and $M_n = 3.5 \times 10^3$ by GPC. The macromolecular initiator then initiated the MPC polymerization with bpy as the ligand, which is the proper synthetic protocol to achieve a moderate reaction rate and proper dispersity on both blocks. After another 12-h reaction, the copolymer solutions were exposed to air to halt the reaction, but the solution still presented a brown color for hours, which means the reaction did not stop immediately.

dx.doi.org/10.1021/am3008399 | ACS Appl. Mater. Interfaces 2012, 4, 4031−4039

Table 1. Elemental Surface Composition of Cellulose Membrane (CM) Substrates Determined from XPS[a]

	element (at. %)					atomic ratio		
sample[b]	C	O	Si	P	N	P/N	Si/C	P/C
pristine	58.89	36.48	3.36	0.26	1.02	0.256	0.057	0.004
14-15	58.30	35.59	2.85	1.61	1.65	0.973	0.049	0.028
14-30	61.68	33.25	1.50	1.69	1.89	0.892	0.024	0.027
14-50	59.33	32.94	3.30	2.17	2.27	0.956	0.056	0.037
14-70	55.34	35.49	5.51	1.74	1.92	0.904	0.100	0.031
14-200	48.02	37.08	11.78	1.57	1.55	1.013	0.245	0.033

[a]Data precision is ~5%. [b]Sample nomenclature format is described in the text (Surface Modification section).

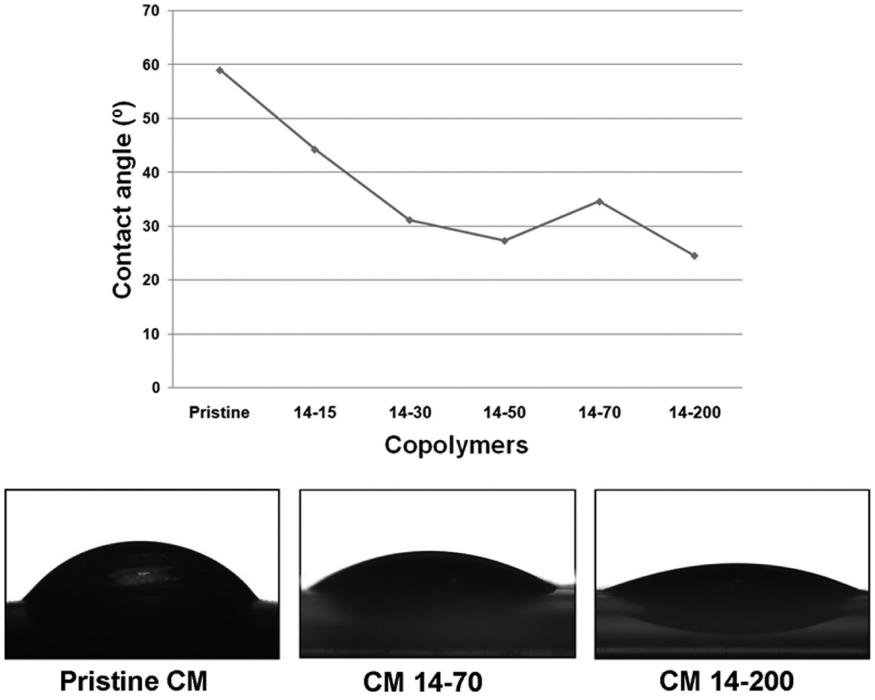

Figure 2. Static contact angle (SCA) pictures and trend graph of the CMs modified with copolymers.

Micelles should form under these conditions, which will be discussed below with the DLS data.

The unpurified products displayed as blue powders when most of the solvent was removed, but they are sensitive to moisture. The interconnection occurred immediately when the final products contacted with moisture in air. The copolymer absorbed the moisture because of hydrophilic PMPC parts, which resulted in the reaction with active sites of PMTSi segments. However, such copolymers are relatively stable in ethanol solutions without any unexpected reactions for months, even with trace of water in solution.

Independent evidence for the micelle formation of the copolymers was obtained from DLS. The intensity size distribution DLS data was acquired from a solution containing copolymers, TEA, and ethanol. The amphiphilic block copolymer can self-assemble to form nanomicelles in alcoholic media. The PMTSi block with low polarity aggregated into a core, while the outer polar PMPC block was present as coronas.[27−29] A bar graph of the d_{mean} value versus copolymers (Figure 1) shows that copolymer 14-50 has the longest mean diameter. In the bar graph of the d_{max} versus copolymers, a proximate linear increase tendency was observed until the degree of MPC polymerization reached 70. Compared to the micelles with similar diameter of the copolymers (from 14-15 to 14-70), composite 14-200 formed the shortest micelles. The phenomena can be ascribed to the different micellization behaviors in solutions. Polar PMPC chain blocks display affinity to ethanol solution, which results in the corona covering the core and a stable micelle formation. Shorter PMPC chains attribute more copolymers aggregating to form larger micelles with lower surface area. Meanwhile, the longer polar chain, which surrounds the core completely, presented the formation of smaller micelles, as well as a smaller entropy increase along the process. The particle size depends on particle volume, length of the polar chain, and the effect of the surfactant group area. Longer length of the polar chains causes smaller particles, although the particle volume remains almost constant.[30] In addition, different micellization patterns would develop distinguished surface morphologies.

Constructing a Phospholipid Polymer Surface on a Cellulose Membrane (CM) via One-Step Modification. The PMTSi moieties possess silanization reactivity. A silanization process is an effective way to chemically change the surface properties of silica-based substrates, because these substrates contain hydroxyl groups that attack and displace the alkoxy groups on the silane-coupling agents, thus forming a covalent C−O−Si bond. Ishihara et al. have synthesized similar copolymers consisting of MPC and MTSi via traditional radical

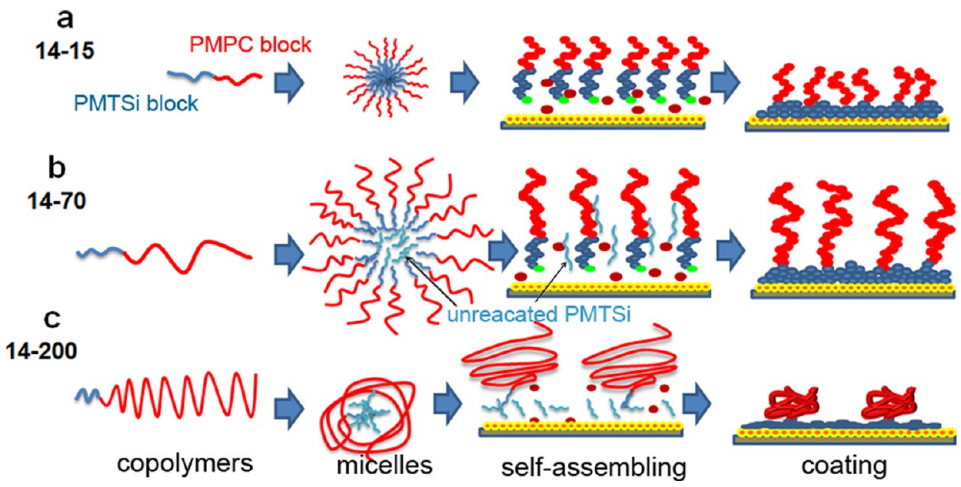

Figure 3. Different surface modification behavior with different PMPC chain length ((a) 14-15, (b) 14-70, and (c) 14-200).

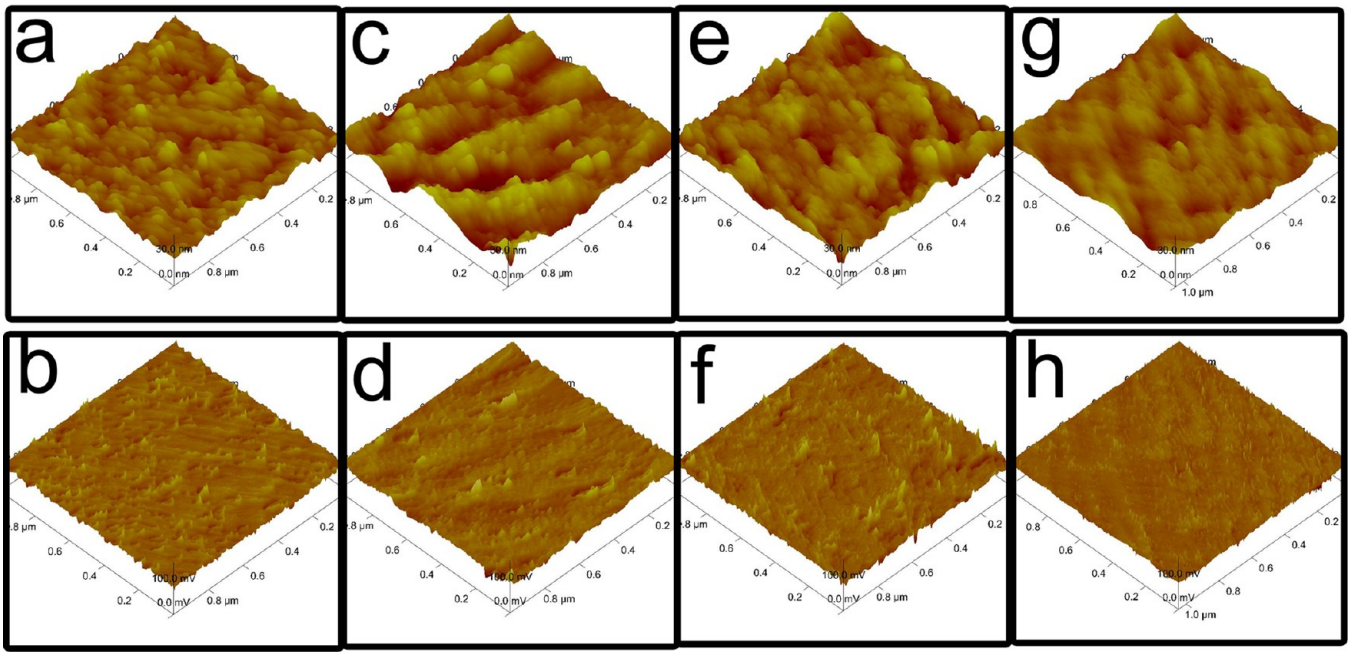

Figure 4. The AFM images of height (1 μm × 1 μm) and amplitude error (1 μm × 1 μm) of (a,b) pristine CM, (c,d) CM modified by 14-15, (e,f) CM modified by 14-70, and CM modified by 14-200 (g,h). The maximum of the bar is 30 nm in height (panels a, c, e, and g) and 100 mV in amplitude error (panels b, d, f, and h).

polymerization. The copolymers designed and synthesized by Ishihara were applied on quartz for protein with different charges adsorption behavior research[7] and microfluids chips.[12] They also coated the copolymers, which were able to construct low-fouling and super lubricated interfaces, onto CLPE (cross-linked polyethylene) for artificial joints[31] and Co−Cr−Mo alloy for orthopedic applications.[32]

The diblock copolymers premade in this paper reacted with CMs, which were widely used in hemodialyzers, gauze, and surgical sutures that come into contact with blood. XPS has been utilized as the method for tracking the surface composition variations of the pristine CMs and CMs modified with different copolymers. Table 1 lists the detailed data from XPS scans on different surfaces.

According to the XPS data (Table 1), the content of carbon almost remains unchanged from pristine CMs to CM 14-50. In CMs 14-70 and 14-200, a decrease in carbon content is presented, which means that diblock copolymers have been attached on the surfaces. The percentage of Si in CMs 14-50 to 14-200 is obviously increased while the content of P and N is similar to that in the other modified samples, which suggests thwat the efficiency of the initiators decreased. When polymerization of the PMPC block proceeded, part of PMTSi-Br macromolecular initiators were aggregated into the core without chain growth. The initiator efficiency increased at first (14-15 and 14-30) and then decreased (14-50, 14-70, and 14-200) with more MPC monomer added in the polymerization system. Longer PMPC chains in polymerization solutions (14-50, 14-70, and 14-200) "imprison" the unreacted PMTSi initiators by using a micelle structure and increasing the solution viscosity. A high concentration of MPC monomer (14-200) rapidly leads to a long chain and the lowest initiator efficiency is attained in the very beginning of the polymerization.

dx.doi.org/10.1021/am3008399 | ACS Appl. Mater. Interfaces 2012, 4, 4031−4039

The ration of P/C reflects the planted MPC block density. In considering of the factors mentioned above, 14-50 modified surfaces show the most PC groups attached on the surface. In contrast, the 14-70 and 14-200 modified surfaces present lower surface density. Compound 14-200 is the longest copolymer with highest composition of PMPC but lowest grafting density. Portions of unreacted PMTSi-Br interconnected with the diblock copolymers and the high Si/C ratio confirmed this phenomenon (14-70, 14-200).

Copolymer solutions with different monomer ratios affected the surface hydrophilicity, surface morphology and biocompatibility. To study the effect of surface modification with different copolymers on hydrophilicity, static water contact angles were measured. A graph of the static contact angle versus copolymers provides more persuasive proof for the points stated above (see Figure 2). The uncoated CM surface is not very hydrophilic, and the decrease in the contact angle after coating indicates that the coating made the surface more hydrophilic than the original surface.. The contact angle of pristine CM, CM 14-70, and 14-200 was 59.0°, 31.3°, and 24.5°, respectively. This phenomenon proved that the wettability of the modified CMs was greatly improved. The PMTSi reacted with the surface hydroxyl and interconnected while the PMPC chains stretched out to form a new layer with high hydrophilicity. Among all of the samples, CMs modified by 14-50 and 14-200 have the best wettability properties. Both PMPC chain length and the branch density, which resulted from the "grafting to" system, accounted for the experimental data. A micelle with proper PMPC chain length should self-assemble onto the cellulose surface by reacting with the hydroxyl groups. Short PMPC chain length results in high branch density and small "mushroom" surface topology; but they are not wide enough to cover the surface or to present a higher static contact angle. In contrast, the longer hydrophilic chains formed a larger "mushroom" morphology and a lower static contact angle (see Figure 3). The 14-50 modified surface holds the most hydrophilic PC groups, as tracked by X-ray photoelectron spectroscopy (XPS) (Table 1), while 14-200 can cover the surface, because of its longest polar chains. Both copolymer-modified CMs can hold more water and present the lowest SCA, which equals better wettability. The 14-70 copolymer modification shows lower surface density, more interconnecting Si−O−Si bonds and longer PMPC chains than 14-50; thus, the SCA was not in the trend.

Surface morphology changes in the membranes were characterized by AFM. As shown in Figure 4, pristine CM (Figures 4a and 4b), and the grafted CM with 14-15 (Figures 4c and 4d), 14-70 (Figures 4e and 4f), 14-200 (Figures 4g and 4h) were investigated. The surface of pristine CM was full of protuberance, the size of which were ~20 nm in height (Figure 4a). CM modified with copolymer 14-15 (Figure 4c) was observed with some larger protuberances (30 nm in height and 150 nm between two ravine-like structures). The original protuberance in size (20 nm) must have been covered with the copolymer 14-15. Copolymer 14-70 (Figure 4e) constructed a novel surface; hemispherical-shaped structures with an approximate height of 15 nm were observed. No ravine-like structures were present any more, either. This phenomenon should be attributed to longer and flexible PMPC chains, reproducing a novel surface. And all the other microstructures formed by silicane and pristine CM chains were also invisible, as confirmed by atomic force microscopy (AFM) photos. Similar to 14-70 modifed surfaces, 14-200 (Figure 4g) surface modification presented a more flat and even morphology. Morphological changes are attributable to the long hydrophilic PMPC block, which induces a significant decrease in surface roughness; this is an important variable for the determination of cellular responses.

The amplitude error photos reflected the "surface hardness" to a certain degree. The PMPC block stretching from the surfaces should lead to a "hard" plot. Copolymer with shorter chains cannot cover the microstructure completely but spread evenly on the surfaces. With limited copolymer "thin layer" modification, the morphology obviously did not change and no "hard" plots were observed (see Figures 4b and 4d). However, copolymers 14-70 and 14-200 with longer PMPC blocks constructed novel surfaces (see Figures 4f and 4h). These long chains can cover the entire surface when stretching but inhomogeneous surfaces can be obtained for a low graft density with a chain block that is too long (14-200) (see Figure 4h). There are a few circular, 8-nm outgrowths spread on the surface modified with 14-200 (see Figure 4h), which are associated with longer PMPC chain and low grafting density. This result is thought to be schematically reasonable, because the grafting density is determined by the distinguished micelle behavior of these diblock copolymers. In this "grafting-to" system, copolymers with long chain modification were prevented by the attached ones from continuous coating for the steric hindrance.[33] Many "hard plots" scattered on the surface where PMPC chains stretched from the surface separately.

Suppressing Biofoulings on Modified Surfaces. The protein adsorption onto a surface depends on the surface properties, to some extent. As described previously, the differences in surface properties of copolymers coating can be essentially attributed to the difference in surface coating density. Hence, it is useful to obtain a relationship between the coating density and the amount of protein adsorbed on the modified surface. As shown in Figure 5, BSA was selected as

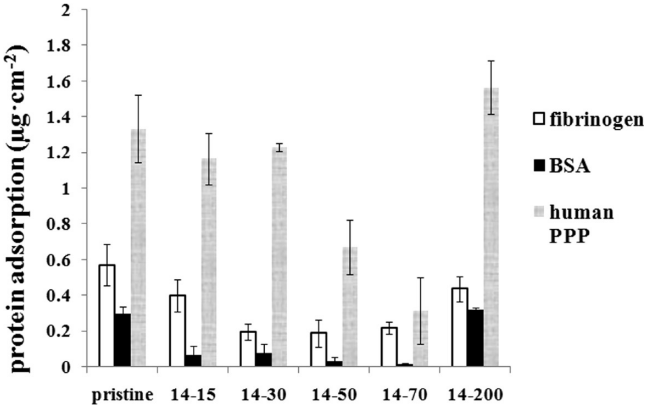

Figure 5. Protein adsorption of series of copolymers (pristine CMs, CMs modified with 14-15, 14-30, 14-50, 14-70; BSA, fibrinogen, human PPP). Data are shown as mean (shaded region) ± standard deviation (SD, shown as error bars), $n \geq 3$).

one of the protein sources for the protein adsorption. The surface coatings remarkably affected protein adsorption. The adsorbed protein amounts on four PMPC copolymer coated surfaces (14-15 to 14-70) were pronouncedly low in general. CM modified with copolymers showed a sensible decrease of the BSA. There is a correlation between protein resistance and polymer layer thickness for PMPC-modified surfaces from 14-15 to 14-70. It is obviously that longer PMPC blocks reduced BSA adsorption more remarkably (14-50, 14-70). However, 14-

200 modified surfaces adsorbed almost the same amount of BSA, compared with pristine CMs. The optimum copolymer in this series was 14-70.

The resistance of modified CMs to protein adsorption was also compared by using fibrinogen and human plasma as protein sources (Figure 5). Fibrinogen adsorption was reduced to one fold on surfaces coated by 14-30, 14-50, and 14-70. Copolymer 14-15 showed a limited effect on fibrinogen adsorption reduction. Moreover, 14-200 showed no effect. In human PPP protein adsorption, 14-70 also presented perfect results. Unlike fibrinogen and BSA solutions, human plasma were complicated in composition, and many sensitive coagulation factors were contained. The amount of protein adsorption remains constant until 14-50 modified CMs. 14-50 and 14-70 modified CMs present obviously less fouling under all conditions, compared with pristine CM. Combining the DLS and AFM data together, PMPC block chain length and graft density together play a decisive role in resistance to protein adsorption degree. Comparing with the high-density coating, the low-density coating has a looser steric structure of coating layer, which may create more chances for some proteins to penetrate into the inner layer of the coating and, consequently, lead to an increase in the amount of protein adsorption. In sum, 14-70, with proper chain length and surface density, can bring in a dense anchor on the CM and a uniform surface modification to achieve a "low-fouling" membrane.[7,33,34]

Figures 6 and 7 shows the platelet adhesion and activation on the membranes. Figure 6 presented the amount of p-selectin

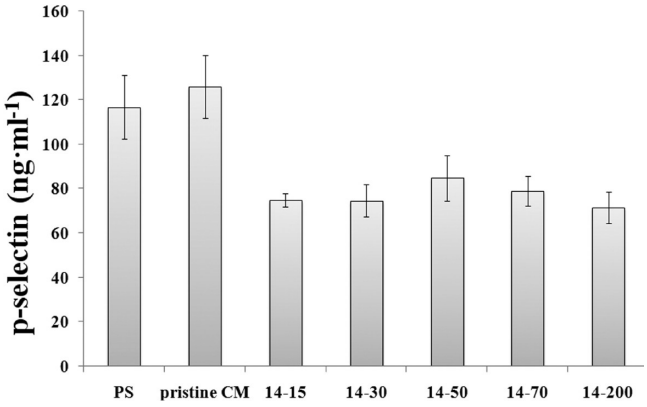

Figure 6. Bar graph showing p-selectin (CD62p) released from PRP in contact with samples. (Samples are polystyrene 24-well tissue plate, pristine CMs, CM modified with 14-15, 14-30, 14-50, 14-70, 14-200. Data are shown as mean ± SD, $n \geq 3$.)

released from the PRP. It is recognized that platelet-mediated mechanisms are the major contributor to thrombosis. Activated platelets express higher levels of the cell surface marker p-selectin, and its release into the blood correlates with biomaterial thrombogenicity.[35] Unlike pristine CMs and PS tissue plates, all of the modified CMs decreased the p-selectin expression. While there are many other contributing factors to thrombosis, including activation of complement, coagulation factors, inflammatory factors, and thrombin, the low platelet activation observed by CMs modified by copolymers is promising.[36]

Figure 7a shows that a few platelets adhered onto the pristine CM, as expected. Some adhered platelets were activated and pseudopodia were extended in Figure 7b. There was almost no platelet adhering on the zwitterionic polymer modified surfaces

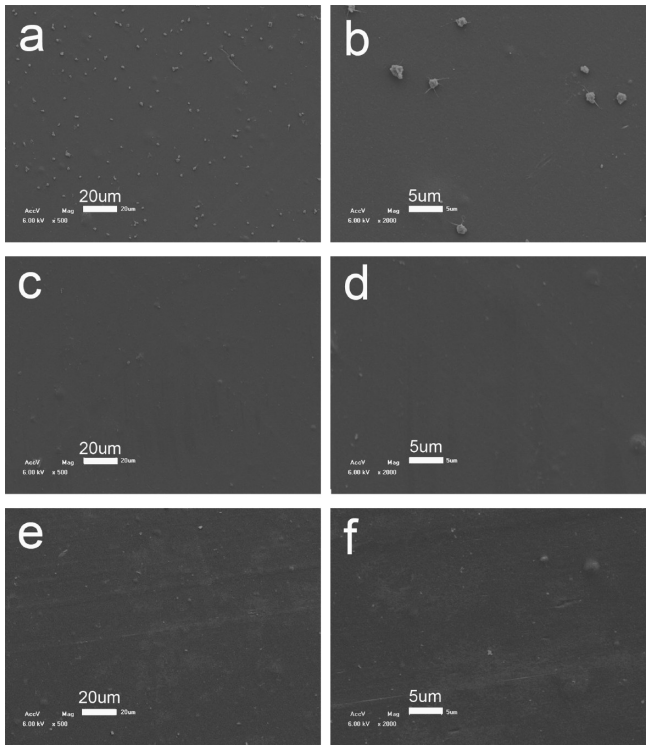

Figure 7. Platelet adhesion on CM ((a,b) pristine, (c,d) modified with 14-70, and (e,f) modified with 14-200).

(Figure 7c–f), indicating that all of the zwitterionic surfaces had excellent resistance to platelet adhesion. However, the result of the platelet adhesion seemed incomplete, in agreement with that of 14-200 protein adsorption results. According to the studies of Barbucci et al.[37] and Ranter et al.,[38] the conformation of the adsorbed fibrinogen, rather than its amount, takes primary responsibility for platelet adhesion and activation. It is believed that the aggregation and adhesion of platelets to materials may depend on the interaction between the exposed "receptor-induced binding site" on conformationally changed fibrinogen and the "ligand-induced binding site" on the platelet membrane. Therefore, although there was a small quantity of proteins adsorbed on the zwitterionic surfaces, the zwitterionic structures could maintain the normal or natural conformation of these adsorbed proteins and, consequently, have less interaction with the platelets.

Copolymer 14-70 has been proved to be the most effective to construct a biocompatible interface. HEK293 cells were cultured to evaluate the surface anticell-adhesion properties. Figure 8 shows a bar graph of cell adhesion on modified and unmodified CMs surfaces on which 293T cells were cultured. The amount adhered on pristine CMs was approximately 1-fold of the amount on polystyrene plates, which implied that CMs is more biocompatible than polystyrene. PMPC copolymer 14-70 modified substrates shows minimal cell adhesion, whereas unmodified substrates exhibited strong cell adhesion. The cell adhesion test confirms that the PMPC surface grafting technique is effective in reducing cell adhesion, and this is widely applied for medical application studies.

■ CONCLUSION

A commercial silicane coupling reagent monomer was used to synthesize a novel functional macromolecular initiator via atomic transfer radical polymerization (ATRP), with DPI =

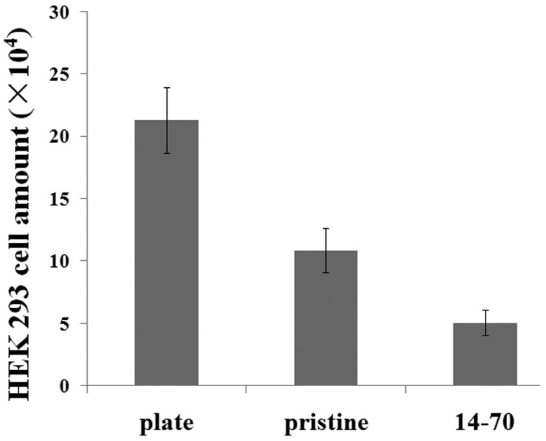

Figure 8. Cell adhesion on plate, pristine CMs, and CMs modified 14-70. Data from four separate experiments are shown as mean ± SD.

1.35 and a number-average molecular weight of M_n = 3500. The biofunctional monomer MPC was then added onto the macromolecular initiators to prepare a series of biocompatible copolymer coatings. Micelles with series sizes and distinguished coating behaviors were observed when the ratio of the two monomers differed. Copolymers with a very long MPC block formed a small micelle. After a convenient "one-step" reaction under mild conditions and a TEA catalyst, cellulose membranes (CMs) were modified by these copolymer solutions. The functional silicane groups reacted with the surface hydroxyl groups and interconnected with each other while the PC groups exposed to air and presented high hydrophilic properties, which was proved by static contact angle (SCA). Surface morphology changes were also monitored by atomic force microscopy (AFM). A homogeneous surface attained under modification by copolymer 14-70. The surface biocompatibility was then tested using BSA, fibrinogen, and plasma as resources. Platelet adhesion and activation also was reduced on all the copolymer coating surfaces. Compared to the protein adsorption amount in different series, 14-70 presented the best effect of all the candidates, which also resisted cell adhesion. Based on the experiments and data above, this novel diblock copolymer promises to be useful in biomedical applications.

AUTHOR INFORMATION

Corresponding Author

*E-mail: chem100@nju.edu.cn (.Q.C.); shenj57@nju.edu.cn (J. S.) .

Notes

The authors declare no competing financial interest.

ACKNOWLEDGMENTS

This research was supported by the National High Technology Research and Development Program of China (No. 2006AA03Z445) and the Changzhou Science and Technology Research Project. It was also supported by Jiangsu Key Laboratory of Biofunctional Materials Project.

REFERENCES

(1) Williams, D. F. *Biomaterials* **2008**, *29*, 2941−2953.
(2) Jang, K.; Sato, K.; Mawatari, K.; Konno, T.; Ishihara, K.; Kitamori, T. *Biomaterials* **2009**, *30*, 1413−1420.
(3) Jang, K.; Sato, K.; Tanaka, Y.; Xu, Y.; Sato, M.; Nakajima, T.; Mawatari, K.; Konno, T.; Ishihara, K.; Kitamori, T. *Lab Chip* **2010**, *10*, 1937−1945.
(4) Fuchs, A. V.; Walter, C.; Landfester, K.; Ziener, U. *Langmuir* **2012**, *28*, 4974−4983.
(5) Wang, C.; Javadi, A.; Ghaffari, M.; Gong, S. *Biomaterials* **2010**, *31*, 4944−4951.
(6) Kim, H. I.; Takai, M.; Ishihara, K. *Tissue Eng. Part C: Methods* **2009**, *15*, 125−133.
(7) Xu, Y.; Takai, M.; Ishihara, K. *Biomacromolecules* **2009**, *10*, 267−274.
(8) Hong, Y.; Ye, S. H.; Nieponice, A.; Soletti, L.; Vorp, D. A.; Wagner, W. R. *Biomaterials* **2009**, *30*, 2457−2467.
(9) Asanuma, Y.; Matsuno, R.; Konno, T.; Takai, M.; Ishihara, K. *Trans. Mater. Res. Soc. Jpn.* **2009**, *34*, 197−200.
(10) Jena, R. K.; Yue, C. Y. *Biomicrofluidics* **2012**, *6*, DOI: 01282210.1063/1.3682098.
(11) Akkahat, P.; Kiatkamjornwong, S.; Yusa, S. I.; Hoven, V. P.; Iwasaki, Y. *Langmuir* **2012**, *28*, 5872−5881.
(12) Xu, Y.; Takai, M.; Konno, T.; Ishihara, K. *Lab Chip* **2007**, *7*, 199−206.
(13) Liu, P. S.; Chen, Q.; Wu, S. S.; Shen, J.; Lin, S. C. *J. Membr. Sci.* **2010**, *350*, 387−394.
(14) Yan, L.; Ishihara, K. *J. Polym. Sci. A: Polym. Chem.* **2008**, *46*, 3306−3313.
(15) Hasegawa, T.; Iwasaki, Y.; Ishihara, K. *J. Biomed. Mater. Res.* **2002**, *63*, 333−341.
(16) Lee, I.; Kobayashi, K.; Sun, H. Y.; Takatani, S.; Zhong, L. G. *J. Biomed. Mater. Res. A* **2007**, *82A*, 316−322.
(17) Wang, Z.; Wan, P.; Ding, M.; Yi, X.; Li, J.; Fu, Q.; Tan, H. *J. Polym. Sci. A: Polym. Chem.* **2011**, *49*, 2033−2042.
(18) Yoon, J. A.; Kowalewski, T.; Matyjaszewski, K. *Macromolecules* **2011**, *44*, 2261−2268.
(19) Feng, W.; Chen, R.; Brash, J. L.; Zhu, S. *Macromol. Rapid Commun.* **2005**, *26*, 1383−1388.
(20) Zhang, Z.; Zhang, M.; Chen, S.; Horbett, T. A.; Ratner, B. D.; Jiang, S. *Biomaterials* **2008**, *29*, 4285−4291.
(21) Rodriguez-Emmenegger, C.; Avramenko, O. A.; Brynda, E.; Skvor, J.; Alles, A. B. *Biosens. Bioelectron.* **2011**, *26*, 4545−4551.
(22) Du, J.; Chen, Y. *Macromolecules* **2004**, *37*, 6322−6328.
(23) Xiong, M.; Zhang, K.; Chen, Y. *Eur. Polym. J.* **2008**, *44*, 3835−3841.
(24) Higuchi, A.; Sugiyama, K.; Yoon, B. O.; Sakurai, M.; Hara, M.; Sumita, M.; Sugawara, S.; Shirai, T. *Biomaterials* **2003**, *24*, 3235−3245.
(25) Kainthan, R. K.; Gnanamani, M.; Ganguli, M.; Ghosh, T.; Brooks, D. E.; Maiti, S.; Kizhakkedathu, J. N. *Biomaterials* **2006**, *27*, 5377−5390.
(26) Seo, J. H.; Matsuno, R.; Konno, T.; Takai, M.; Ishihara, K. *Biomaterials* **2008**, *29*, 1367−1376.
(27) Liu, G.; Jin, Q.; Liu, X.; Lv, L.; Chen, C.; Ji, J. *Soft Matter* **2011**, *7*, 662−669.
(28) Yu, B.; Lowe, A. B.; Ishihara, K. *Biomacromolecules* **2009**, *10*, 950−958.
(29) Giacomelli, C.; Le Men, L.; Borsali, R.; Lai-Kee-Him, J.; Brisson, A.; Armes, S. P.; Lewis, A. L. *Biomacromolecules* **2006**, *7*, 817−828.
(30) Correa, N. M.; Silber, J. J.; Riter, R. E.; Levinger, N. E. *Chem. Rev.* **2012**, DOI: 10.1021/cr200254q.
(31) Kyomoto, M.; Moro, T.; Miyaji, F.; Hashimoto, M.; Kawaguchi, H.; Takatori, Y.; Nakamura, K.; Ishihara, K. *J. Biomed. Mater. Res. A* **2009**, *90A*, 362−371.
(32) Kyomoto, M.; Moro, T.; Iwasaki, Y.; Miyaji, F.; Kawaguchi, H.; Takatori, Y.; Nakamura, K.; Ishihara, K. *J. Biomed. Mater. Res. A* **2009**, *91A*, 730−741.
(33) Yoshimoto, K.; Hirase, T.; Madsen, J.; Armes, S. P.; Nagasaki, Y. *Macromol. Rapid Commun.* **2009**, *30*, 2136−2140.
(34) Unsworth, L. D.; Sheardown, H.; Brash, J. L. *Langmuir* **2005**, *21*, 1036−1041.
(35) Motlagh, D.; Yang, J.; Lui, K. Y.; Webb, A. R.; Ameer, G. A. *Biomaterials* **2006**, *27*, 4315−4324.

(36) Waterhouse, A.; Yin, Y.; Wise, S. G.; Bax, D. V.; McKenzie, D. R.; Bilek, M. M. M.; Weiss, A. S.; Ng, M. K. C. *Biomaterials* **2010**, *31*, 8332−8340.
(37) Xu, Y.; Takai, M.; Ishihara, K. *Biomaterials* **2009**, *30*, 4930−4938.
(38) Barbucci, R.; Lamponi, S.; Magnani, A. *Biomacromolecules* **2003**, *4*, 1506−1513.